Cell Reports
Medicine

Article

A polyamine-centric, blood-based metabolite panel predictive of poor response to CAR-T cell therapy in large B cell lymphoma

Graphical abstract

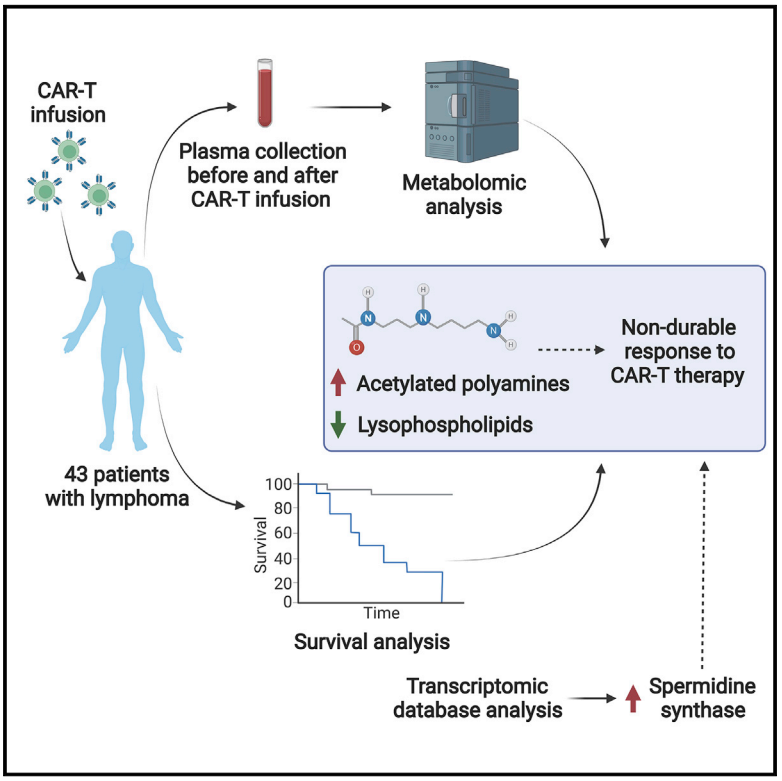

Highlights

- Plasma acetylated polyamines are predictive of poor response to CAR-T therapy
- Tumoral SRM gene expression is prognostic for poor survival in r/r LBCL
- A 6-marker metabolite panel was developed to predict response to CAR-T therapy

Authors

Johannes F. Fahrmann, Neeraj Y. Saini, Chang Chia-Chi, ..., Marion Subklewe, Sattva S. Neelapu, Sam Hanash

Correspondence

marion.subklewe@med.uni-muenchen.de (M.S.), sneelapu@mdanderson.org (S.S.N.), shanash@mdanderson.org (S.H.)

In brief

Fahrmann et al. report a blood-based metabolite panel that identifies patients with relapsed or refractory large B cell lymphoma (r/r LBCL) who are unlikely to respond to anti-CD19 CAR T-cell therapy. The metabolite panel in combination may provide a useful tool for the management of patients with r/r LBCL.

Fahrmann et al., 2022, Cell Reports Medicine *3*, 100720
November 15, 2022
https://doi.org/10.1016/j.xcrm.2022.100720

CellPress

Cell Reports Medicine

CellPress
OPEN ACCESS

Article

A polyamine-centric, blood-based metabolite panel predictive of poor response to CAR-T cell therapy in large B cell lymphoma

Johannes F. Fahrmann,[1,11] Neeraj Y. Saini,[2,3,11] Chang Chia-Chi,[8] Ehsan Irajizad,[1,4] Paolo Strati,[3] Ranjit Nair,[3] Luis E. Fayad,[3] Sairah Ahmed,[3] Hun Ju Lee,[3] Swaminathan Iyer,[3] Raphael Steiner,[3] Jody Vykoukal,[1] Ranran Wu,[1] Jennifer B. Dennison,[1] Loretta Nastoupil,[3] Preetesh Jain,[3] Michael Wang,[3] Michael Green,[3] Jason Westin,[3] Viktoria Blumenberg,[5,6] Marco Davila,[7] Richard Champlin,[2] Elizabeth J. Shpall,[2] Partow Kebriaei,[2] Christopher R. Flowers,[3] Michael Jain,[7] Robert Jenq,[8] Christoph K. Stein-Thoeringer,[6,9] Marion Subklewe,[5,9,10,*] Sattva S. Neelapu,[3,*] and Sam Hanash[1,12,*]

[1]Department of Clinical Cancer Prevention, The University of Texas MD Anderson Cancer Center, 6767 Bertner Avenue, Houston, TX 77030, USA
[2]Department of Stem Cell Transplantation and Cellular Therapy, The University of Texas MD Anderson Cancer Center, 1515 Holcombe Boulevard, Houston, TX 77030, USA
[3]Department of Lymphoma and Myeloma, The University of Texas MD Anderson Cancer Center, 1515 Holcombe Boulevard, Houston, TX 77030, USA
[4]Department of Biostatistics, The University of Texas MD Anderson Cancer Center, 6767 Bertner Avenue, Houston, TX 77030, USA
[5]Department of Medicine III, University Hospital, LMU Munich, 81377 Munich, Germany
[6]National Center for Tumor Diseases (NCT), Neuenheimer Feld 460, 69120 Heidelberg, Germany
[7]Department of Blood and Marrow Transplant and Cellular Therapy, Moffitt Cancer Center, 12902 USF Magnolia Drive, Tampa, FL 33612, USA
[8]Department of Genomic Medicine, The University of Texas MD Anderson Cancer Center, 1515 Holcombe Boulevard, Houston, TX 77030, USA
[9]German Cancer Research Center (Deutsches Krebsforschungszentrum, DKFZ), Heidelberg, Germany
[10]Laboratory for Translational Cancer Immunology, Gene Center of the LMU Munich, Munich, Germany
[11]These authors contributed equally
[12]Lead contact
*Correspondence: marion.subklewe@med.uni-muenchen.de (M.S.), sneelapu@mdanderson.org (S.S.N.), shanash@mdanderson.org (S.H.)
https://doi.org/10.1016/j.xcrm.2022.100720

SUMMARY

Anti-CD19 chimeric antigen receptor (CAR) T cell therapy for relapsed or refractory (r/r) large B cell lymphoma (LBCL) results in durable response in only a subset of patients. MYC overexpression in LBCL tumors is associated with poor response to treatment. We tested whether an MYC-driven polyamine signature, as a liquid biopsy, is predictive of response to anti-CD19 CAR-T therapy in patients with r/r LBCL. Elevated plasma acetylated polyamines were associated with non-durable response. Concordantly, increased expression of spermidine synthase, a key enzyme that regulates levels of acetylated spermidine, was prognostic for survival in r/r LBCL. A broad metabolite screen identified additional markers that resulted in a 6-marker panel (6MetP) consisting of acetylspermidine, diacetylspermidine, and lysophospholipids, which was validated in an independent set from another institution as predictive of non-durable response to CAR-T therapy. A polyamine centric metabolomics liquid biopsy panel has predictive value for response to CAR-T therapy in r/r LBCL.

INTRODUCTION

The use of adoptively transferred T cells modified with chimeric antigen receptor (CAR) has heralded a new era in the treatment of large B cell lymphoma (LBCL) for patients with relapsed or refractory (r/r) LBCL.[1–4] Three CD19-CAR-T cell products are approved for r/r LBCL—axicabtagene ciloleucel,[2] tisagenlecleucel,[3] and lisocabtagene maraleucel.[4] However, despite remarkable overall response rates (ORRs), long-term durability of responses with these therapies was only observed in approximately 30%–40% of patients.[2–4]

Currently, there is a paucity of biomarkers that can predict patients with LBCL who are unlikely to achieve durable responses with CAR-T cell therapy. Prior studies have shown that biomarkers, such as elevated lactate dehydrogenase (LDH) levels, that serve as a measure of tumor burden, c-reactive protein (CRP), increased tumor interferon signaling, and elevated interleukin-6 (IL-6) at baseline are associated with increased risk of early disease progression after CAR-T cell therapy in r/r LBCL.[3,5,6] However, external validation of these findings has been limited. Thus, there is a need for additional biomarkers to identify patients with LBCL at high risk of relapse after CAR-T cell therapy.

Table 1. Patient and tumor characteristics and incidence of CRS and ICANS in the test and validation cohorts

	Test set		Validation set	
	Ongoing CR[a]	PD/PR[a]	Ongoing CR[b]	PD[b]
Participants, N	15	28	11	17
Age, mean ± SD	57 ± 16	60 ± 12	65 14	55 ± 15
Gender, N (%)				
Female	2 (13)	11 (39)	7 (64)	5 (29)
Male	13 (87)	17 (61)	4 (36)	12 (71)
Disease type, N (%)				
DLBCL	13 (87)	21 (75)	8 (73)	13 (76)
TFL	2 (13)	7 (25)	–	–
MCL	–	–	2 (18)	2 (12)
tCLL	–	–	–	1 (6)
BCP-ALL	–	–	1 (9)	1 (6)
Stage, N (%)				
I–II	4 (27)	5 (18)	4 (36)	4 (23)
III–IV	11 (73)	23 (82)	6 (55)	12 (71)
Unknown	–	–	1 (9)	1 (6)
Bulky disease, N (%)				
< 10cm	8 (53)	20 (71)	–	–
≥ 10cm	3 (20)	3 (11)	–	–
Unknown	4 (27)	5 (18)	–	–
ABC/GCB status, N (%)				
ABC	3 (20)	7 (25)	–	–
GCB	7 (47)	16 (57)	–	–
Unknown	5 (33)	5 (18)	–	–
Bcl-2/Bcl-6 expressors, N (%)				
No	5 (33)	9 (32)	–	–
Yes	5 (33)	11 (39)	–	–
Unknown	5 (33)	8 (29)	–	–
Double/Ttiple Hit[c], N (%)				
No	9 (60)	15 (54)	–	–
Yes	1 (7)	7 (25)	–	–
Unknown	5 (33)	6 (21)	–	–
ECOG at day 0, N (%)				
0	3 (20)	5 (18)	4 (36)	2 (12)
1	8 (53)	20 (71)	7 (64)	8 (47)
2	4 (27)	1 (4)	–	4 (23)
3	–	2 (7)	–	3 (18)
IPI score				
0	1 (7)	1 (4)	–	–
1	3 (20)	4 (14)	–	–
2	6 (40)	7 (25)	–	–
3	3 (20)	10 (36)	–	–
4	2 (13)	6 (21)	–	–
LDH (U/L) at day 0, mean ± SD	276 ± 110	341 ± 192	231 ± 86	423 ± 286
CRS grade, N (%)				
0	1 (7)	2 (7)	–	2 (12)
1	8 (53)	14 (50)	7 (64)	7 (41)
2	6 (40)	10 (36)	3 (27)	5 (29)

(*Continued on next page*)

Table 1. *Continued*

	Test set		Validation set	
	Ongoing CR[a]	PD/PR[a]	Ongoing CR[b]	PD[b]
3	–	1 (4)	1 (9)	3 (18)
4	–	1 (4)	–	–
ICANs grade, N (%)				
0	8 (53)	11 (39)	4 (36)	10 (59)
1	1 (7)	4 (14)	4 (36)	5 (29)
2	2 (13)	2 (7)	2 (18)	1 (6)
3	3 (20)	7 (25)	–	1 (6)
4	1 (7)	4 (14)	1 (9)	–

CR, complete response; PD, progressive disease; PR, partial response; DLBCL, diffuse large B cell lymphoma; TFL, transformed follicular lymphoma; MCL, mantle cell lymphoma; tCLL, T cell chronic lymphocytic leukemia; BCP-ALL, B cell precursor acute lymphoblastic leukemia; ABC, activated B cell; GBC, germinal center B cell; ECOG, Eastern Cooperative Oncology Group; IPI, International Prognostic Index; LDH, lactate dehydrogenase; CRS, cytokine release syndrome; ICANS, immune effector cell-associated neurotoxicity syndrome.
[a]Based on 6 month follow-up period.
[b]Based on 3 month follow-up period.
[c]*MYC* plus *Bcl-2* and/or *Bcl-6* rearrangements.

MYC is an oncogenic driver of LBCL pathogenesis.[7,8] Recent findings from the JULIET trial suggest that baseline MYC overexpression in r/r diffuse DLBCL (DLBCL) tumors is inversely associated with durable response to CAR-T cell therapy.[9] Oncogenic MYC regulates transcription of several polyamine metabolizing enzymes, resulting in increased levels of circulating polyamines.[10–12]

Here, we tested the utility of plasma polyamines for predicting poor response to CAR-T cell therapy as part of a comprehensive plasma metabolomics profiling and observed elevated levels of several polyamines to be associated with worse progression-free survival (PFS) and overall survival (OS). Comprehensive metabolomics profiling resulted in a panel consisting of polyamines and lysophospholipids, which was validated in an independent set for prediction of poor response to CAR-T therapy among patients with r/r LBCL.

RESULTS

Identification of predictive metabolite signatures and model development

A test cohort consisting of plasma samples collected within 4 days preceding anti-CD19 CAR-T cell therapy from 43 patients with r/r LBCL at the MD Anderson Cancer Center was assembled to test the performance of polyamines and other metabolites as potentially predictive of response to CAR-T cell therapy (test set). Baseline patient and tumor characteristics are provided in Table 1. Patients were treated with either axicabtagene ciloleucel (N = 39) or tisagenlecleucel (N = 4). The median duration of follow up in the test cohort was 11 months (range 0.5–27.6 months). Median PFS was 4 months (Figure S1). Three patients died early due to adverse events prior to response assessment at day 30. Among the 40 evaluable patients, 15 (37%) had an ongoing complete response (CR), one had an ongoing partial response (PR) at 6 months of follow up, and 24 (60%) had progressive disease (PD).

Four plasma polyamines (acetylspermidine [AcSpmd], diacetylspermidine [DiAcSpmd], diacetylspermine [DAS], and N-(3-acetamidopropyl)pyrrolidin-2-one)) were detected and quantified (Table S1). Cox proportional hazard models revealed that elevated levels of the polyamines AcSpmd, DiAcSpmd, and DAS were associated with worse PFS and OS (Figure 1A). At 95% specificity, AcSpmd, DiAcSpmd, and DAS had resultant sensitivities of 17.9%, 32.1%, and 21.4%, respectively, at 95% for identifying patients who had PD/PR or who died within 6 months post CAR-T cell treatment (Table S2). Plasma levels of acetylated polyamines, particularly DAS, were positively correlated with tumor staining for MYC (Table S3). We further assessed intra-patient levels of AcSpmd, DiAcSpmd, and DAS up to 16 days post CAR-T cell infusion, the results of which showed that polyamines remained high in patients who had PD/PR or who died within 6 months post CAR-T cell treatment compared with those with an ongoing CR (Figure 2).

Complementary to the three polyamines (AcSpmd, DiAcSpmd, and DAS), untargeted metabolomic analyses of these plasma samples yielded an additional 746 annotated metabolite features. Of these, 56 additional metabolites other than polyamines were found to be statistically significantly (2-sided $p < 0.05$) associated with PFS, and 19 metabolites were prognostic for OS, of which 15 were prognostic for both PFS and OS (Table S1). In the case of individual lipid species, to mitigate non-specificity due to external factors such as dietary patterns or randomness, emphasis was given to those lipids that showed uniformity in the performance characteristics among the entire lipid class (i.e., >80% of the detected individual lipids in each lipid class exhibited concordant associations with clinical outcomes). On this basis, we found that several cancer-relevant lysophospholipids[10,13,14] were associated with worse survival outcomes (Figure 1).

Cox proportional hazard models with LASSO regularization were used to select predictive metabolites, which resulted in a 6-marker metabolite panel (6MetP) consisting of AcSpmd, DiAcSpmd on the basis of their increased levels, and four lysophospholipids (lysophosphatidylcholine [16:0], lysophosphatidylcholine [14:0], plasmanyl-lysophosphatidycholines [P-18:0 or O-18:1], and plasmanyl-lysophosphatidycholine [P-18:1 or O-18:2]) on the basis of their reduced levels for predicting PFS.

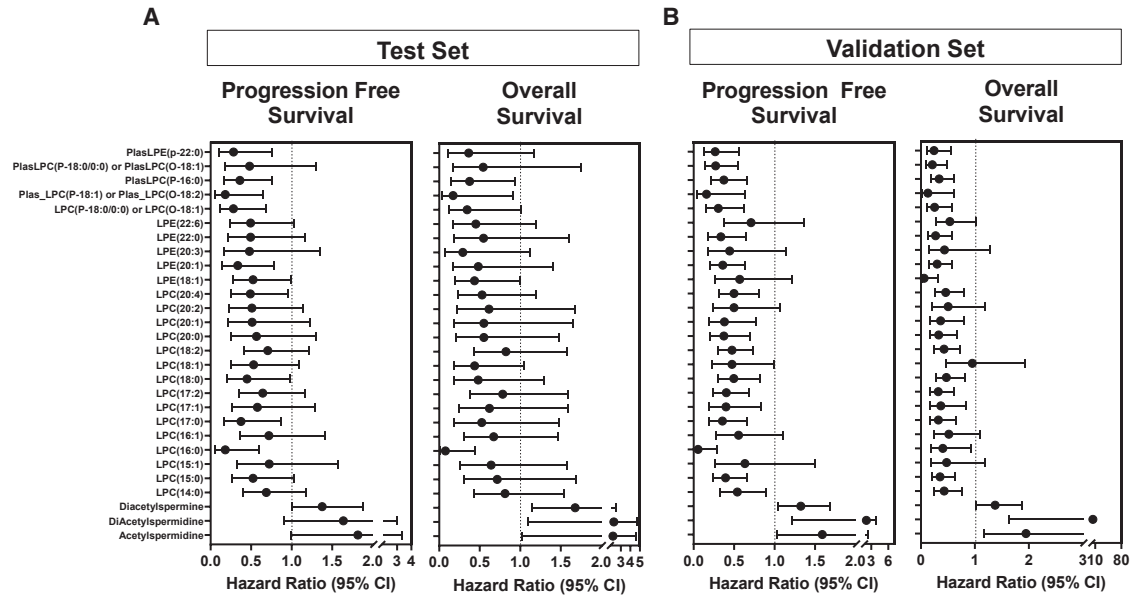

Figure 1. Association between circulating lysophospholipids and polyamines with progression-free survival and overall survival in patients with B cell lymphoma treated with CAR-T

(A and B) Dot plots represent hazard ratios (HRs) (95% CI) per unit increase in log2 scale of detected polyamines and lysophospholipids for progression-free survival (PFS) and overall survival (OS) in the test set (A) and the validation set (B).

In multivariable Cox proportional hazard models, adjusting for other significant (1-sided $p < 0.05$) variables, the 6MetP score yielded a hazard ratio (HR) of 3.65 (95% confidence interval [CI]: 1.38–9.67) per unit increase (Table S4). Assumptions of Cox proportional hazard were met in our model.

The 6MetP panel had an area under the receiver operating characteristic curve of 0.79 (95% CI: 0.65–0.93) with 40% sensitivity at 95% specificity for discriminating patients who had PD/PR or who died within 6 months post CAR-T cell treatment from those that had an ongoing CR (Figure 3A and S2). Next, using log rank test statistics from the Cox model, we calculated an optimal change point for the 6MetP score to yield the greatest difference between individuals in the two already defined groups (disease progression versus no disease progression) (Figure S3). Kaplan-Meier survival curves revealed that patients with 6MetP scores above the cutoff value had statistically significantly worse PFS and worse OS (Figure 4A log rank Mantel Cox test 2-sided $p < 0.001$). No statistically significant association was observed between the 6MetP score and cytokine release syndrome (CRS) or immune effector cell-associated neurotoxicity syndrome (ICAN) toxicity (data not shown).

Testing of the metabolite biomarker panel in an independent validation set

Validation of individual candidate metabolites as well as of the 6MetP using fixed model coefficients and cutoff values for predicting PFS following anti-CD19 CAR-T cell treatment was performed in an independent validation set consisting of serum samples from 28 patients with r/r LBCL who subsequently received anti-CD19 CAR-T cell therapy (Table 1). The median duration of follow up in the validation cohort was 12 months (range 0.3–24.8 months). In the validation set, 11 (39%) of the 28 patients had an ongoing CR at 6 months of follow up, whereas the other 17 (61%) patients had PD or died. Median PFS and OS among non-responders was 2.9 and 8.25 months, respectively (Figure S1).

In the validation set, elevated circulating polyamines were associated with poor PFS and poor OS, as was the case for reduced levels of lysophospholipids (Figure 1B). The fixed 6MetP yielded an area under the receiver operating characteristic curve (AUC) of 0.71 (95% CI: 0.52–0.90) with 41% sensitivity at 95% specificity for distinguishing patients who relapsed or died within 6 months post CAR-T cell treatment from those patients who had an ongoing CR (Figure 3B and S2). In multivariable analyses, when considering other variables that were statistically significantly associated with PFS, the fixed 6MetP score as a continuous variable was independently associated with worse PFS (HR: 2.31 [95% CI: 1.05–5.05]) (Table S5). A 6MetP score above the cutoff value that was established in the test set was found to be a statistically significant (log rank Mantel Cox test 1-sided $p < 0.05$) prognostic indicator of worse PFS as well as OS in the validation set (Figure 4B).

mRNA expression of polyamine metabolizing enzymes is prognostic in B cell lymphomas and is associated with reduced tumor immune cell infiltrates.

Our analyses revealed that elevated levels of circulating polyamines are prognostic for poor PFS and OS among patients receiving CAR-T cell therapy. We assessed whether the circulating polyamine signature may be accounted for based on increased expression of polyamine synthesizing enzymes in LBCL tumors. We analyzed the Basso lymphoma gene-expression dataset[16] and found that mRNA expression of enzymes central to polyamine metabolism were statistically significantly higher (Wilcoxon rank sum test 2-sided $p < 0.05$) in DLBCL cells compared with healthy B lymphocytes (Figure 5A). Next, we assessed for association

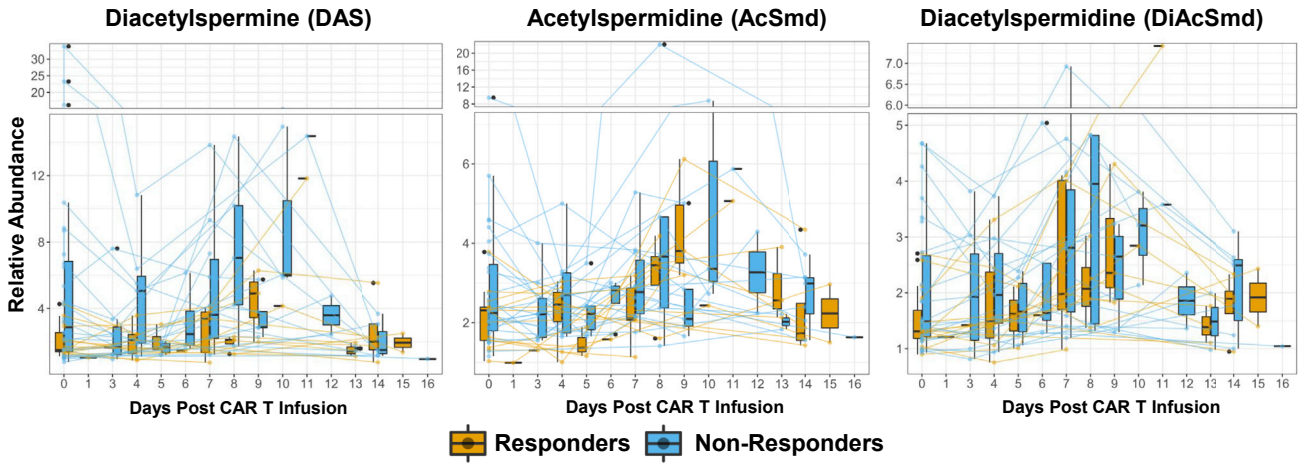

Intra-patient slopes considering random variables for intercept and slope			
Metabolite	**Responders**	**Non-Responders**	**Pval**
DAS	-0.077 (-0.107 to -0.065)	0.086 (0.062 to 0.115)	<0.0001
AcSpmd	0.028 (0.013 to 0.048)	0.074 (0.057 to 0.087)	<0.0001
DiAcSpmd	0.034 (0.020 to 0.034)	0.069 (0.057 to 0.078)	<0.0001

Figure 2. Circulating polyamine levels post CAR-T cell infusion in patients with r/r LBCL

Linear mixed models with random intercept and slope were incorporated to calculate the association between polyamine levels following CAR-T infusion. Reported values (slope and intercepts) in the table are the average representation of all calculated coefficients for each patient. p values were calculated from 10,000 bootstraps of the delta value between responders and non-responders.

between gene expression of these polyamine metabolizing enzymes (PMEs) and PFS in the TCGA-DLBCL dataset. Of the PMEs, elevated mRNA expression of spermidine synthase (SRM) was identified as a statistically significant poor-prognostic indicator of PFS (Figures 5B and 5C). Analysis of two additional independent B cell lymphoma transcriptomic datasets[17,18] similarly revealed elevated gene expression of SRM in LBCLs to be associated with statistically significantly worse OS (Figures 5B and 5C). Thus, elevated plasma polyamines reflect increased mRNA expression of PMEs in tumor samples, both of which are associated with poor prognosis in B cell lymphoma.

Using the TCGA-DLBCL and the Ma[19] DLBCL transcriptomic datasets, we additionally assessed the relationship between gene expression of PMEs and the tumor immunophenotype and found that elevated mRNA levels of the PMEs ornithine decarboxylase 1 (*ODC1*), *SRM*, and spermine synthase (*SMS*) were consistently negatively correlated with immune-checkpoint-blockade-related genes including cytotoxic T lymphocyte-associated protein 4 (*CTLA4)* and programmed cell death 1 (*PD-1)* as well as gene-based signatures of regulatory T cells (Tregs), T helper 17 (Th17) cells, T follicular helper (Tfh) cells, natural killer cells, and eosinophils (Figure 5D; Tables S4, S6, and S7), suggesting that LBCLs with elevated polyamine metabolism may exhibit low immune infiltration.

DISCUSSION

Only a subset of patients with r/r LBCL receiving anti-CD19 CAR-T cell therapy will achieve a durable response, with over half of the patients exhibiting disease relapse by 12 months after treatment.[21] The paucity of biomarkers that can predict durable responses is a significant limiting factor for the individualized management of patients undergoing treatment with CAR-T cell therapy. We tested the hypothesis that altered polyamine metabolism in LBCL may lead to a predictive liquid biopsy marker combination. We used a training and validation approach to interrogate the circulating metabolome and develop a metabolite panel consisting of AcSpmd, DiAcSpmd, and lysophospholipids that is predictive of poor response to anti-CD19 CAR-T cell treatment and that identifies patients at high risk of disease progression. Importantly, when adjusting for other known risk factors including Eastern Cooperative Oncology Group (ECOG) status[22] and circulating LDH levels,[5] the 6MetP score remained an independent prognostic indicator of poor PFS following CAR-T cell treatment.

MYC overexpression in r/r DLBCL tumors prior to CAR-T therapy has been reported to be negatively associated with durable response to CAR-T cell therapy.[9] In our study, MYC overexpression in r/r DLBCL showed a tendency to be associated with poor response to CAR-T therapy. Polyamine metabolism upregulation through oncogenic MYC is a common metabolic irregularity in aggressive cancers, including lymphomas.[11,23,24] Specifically, MYC is an established transcriptional regulator of PMEs, including ODC1, SRM, and SMS, that yield non-acetylated polyamines. The catabolism of polyamines to their acetylated derivatives is mediated by spermidine/spermine N1-acetyltransferase 1 (SAT1), which is responsive to intra-cellular polyamine levels.[11,25] Here, we provide evidence that acetylated polyamines in the

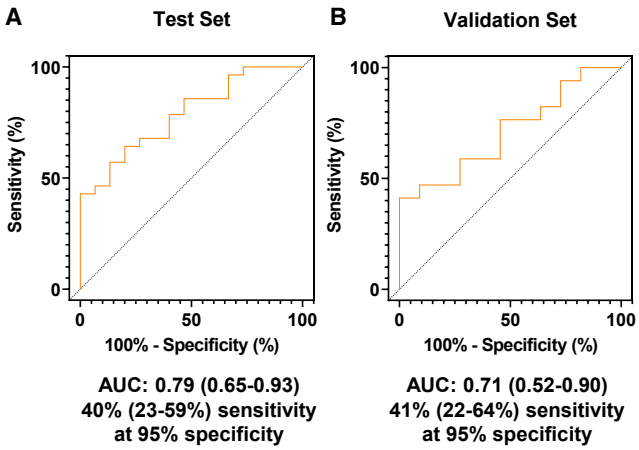

Figure 3. Predictive performance of the 6-marker metabolite panel (6MetP) for CAR-T cell response in the test and validation set

(A and B) AUC curves are shown using the 6MetP scores for distinguishing patients who had who progressive disease or died within 6 months following CAR T cell treatment from those patients who had an ongoing complete response in the test set (A) and the validation set (B).

blood are predictive of non-durable response to CAR-T cell therapy in patients with r/r DLBCL. Moreover, our data suggest that circulating acetylated polyamine levels may function as a better predictor of therapeutic outcome to CAR-T cell therapy compared with upstream MYC expression.

We additionally provide evidence that elevations in circulating polyamines are associated with LBCL tumors that are characterized by low immune cell infiltrate. In prior studies of triple-negative breast cancer, we reported an association between plasma DAS and tumor spermine synthase with outcome.[11] A lack or paucity of infiltrating T cells in tumors with elevated levels of PMEs attenuates efficacy of immunotherapies, including CAR-T cell therapy.[26] Similarly, decreased antigen expression before CAR-T cell treatment or antigen loss or antigen-low escape following CAR-T cell treatment are associated with CAR-T cell therapy resistance.[27] Mechanistically, excessive production and absorption of polyamines from the microenvironment by cancer cells promotes their proliferation and immune evasion.[28–30] Recently, Jain and colleagues showed that myeloid-derived suppressor cells (MDSCs) and higher IL-6 cytokine levels are associated with reduced CAR-T cell expansion and poor anti-lymphoma responses after anti-CD19 CAR-T cell therapy.[6] Polyamines have been reported to increase MDSCs and lead to an immunosuppressive tumor microenvironment.[31] Moreover, polyamines have been shown to be important for effector function of several immune cell types including T cells.[32–34] Collectively, this suggest a possible pathophysiologic mechanism by which polyamines could dampen the effect of CAR-T cell therapy and support development of therapeutic strategies to target polyamine metabolism and uptake using agents, such as the small-molecule ODC1 inhibitor difluoromethylornithine (DFMO) or the polyamine transporter inhibitor AMXT-1501, to augment the efficacy of CAR-T cell therapy.[35,36]

Lysophopholipids, particularly lysophosphatidycholines, are bioactive lipids that are scavenged and metabolized by cancer cells to promote cancer cell growth.[10,37,38] Decreased levels of lysophospholipids are frequently reported in plasma of individuals presenting with various malignancies including pancreas, lung, ovarian, and colorectal cancers.[10,13,14] Metabolic plasticity of T cells is crucial to maintain high invasion potential and cytotoxic function. To this end, prior studies have shown that the lysophosphatidylcholine (LPC)-scavenging receptor MFSD2A is highly expressed in activated T cells and memory T cells, and transient increases in intra-cellular LPCs parallels and potentiates T cell activation.[32,39,40] Conditional loss of MFSD2A in $CD8^+$ T cells was shown to reduce LPC uptake, resulting in attenuated effector function and reduced memory T cell formation and maintenance.[39] Therefore, it is likely that lower bioavailability of circulating lysophospholipids may diminish proliferation and functions of CAR-T cells, resulting in lower clinical efficacy. Prior studies have demonstrated that targeting lysophospholipid metabolism using edelfosine, a synthetic alkyl-lysophopholipid, exerts preferential toxicity to cancer cells.[41–43] Edelfosine may thus provide another potential strategy for enhancing efficacy of CAR-T treatment.

There are some limitations of our study. We found that elevated tumoral gene expression of SRM is associated with poor prognosis in lymphomas regardless of CAR-T cell treatment. This suggests that increased plasma acetylated polyamine levels may indicate an aggressive manifestation of LBCL that is less likely to respond to CAR-T cell therapy. Nevertheless, the primary translational goal of the current study was to identify and establish a clinically relevant metabolite panel that predicts response to CAR-T treatment in r/r LBCL. Here, we report a metabolite panel for risk of non-durable response to CAR-T therapy among patients with r/r LBCL. While the size of the available cohorts described in our study was limited, our independent validation of the fixed 6MetP score and derived cutoffs in samples from an independent site provides confidence in the findings. Moreover, we provide plausible mechanism consistent with the state of the field, although we acknowledge that further investigations will be needed to define the detailed mechanism(s) by which metabolite features impact response to CAR-T treatment. With CAR-T therapy being increasingly explored as a frontline treatment for lymphoma, it remains to be determined whether the metabolite panel can also identify individuals with newly diagnosed lymphoma who are unlikely to respond to CAR-T therapy.

In conclusion, we established a blood-based metabolite panel that identifies patients who are less likely to respond to anti-CD19 CAR-T cell treatment and who are at high risk of lymphoma progression. Further validation of our 6MetP for predicting non-response to CAR-T cell treatment and poor prognosis is warranted in a larger sample size. The 6MetP, in combination with other established risk markers,[5] may provide a useful tool for the management of patients with r/r LBCL.

STAR★METHODS

Detailed methods are provided in the online version of this paper and include the following:

- KEY RESOURCES TABLE

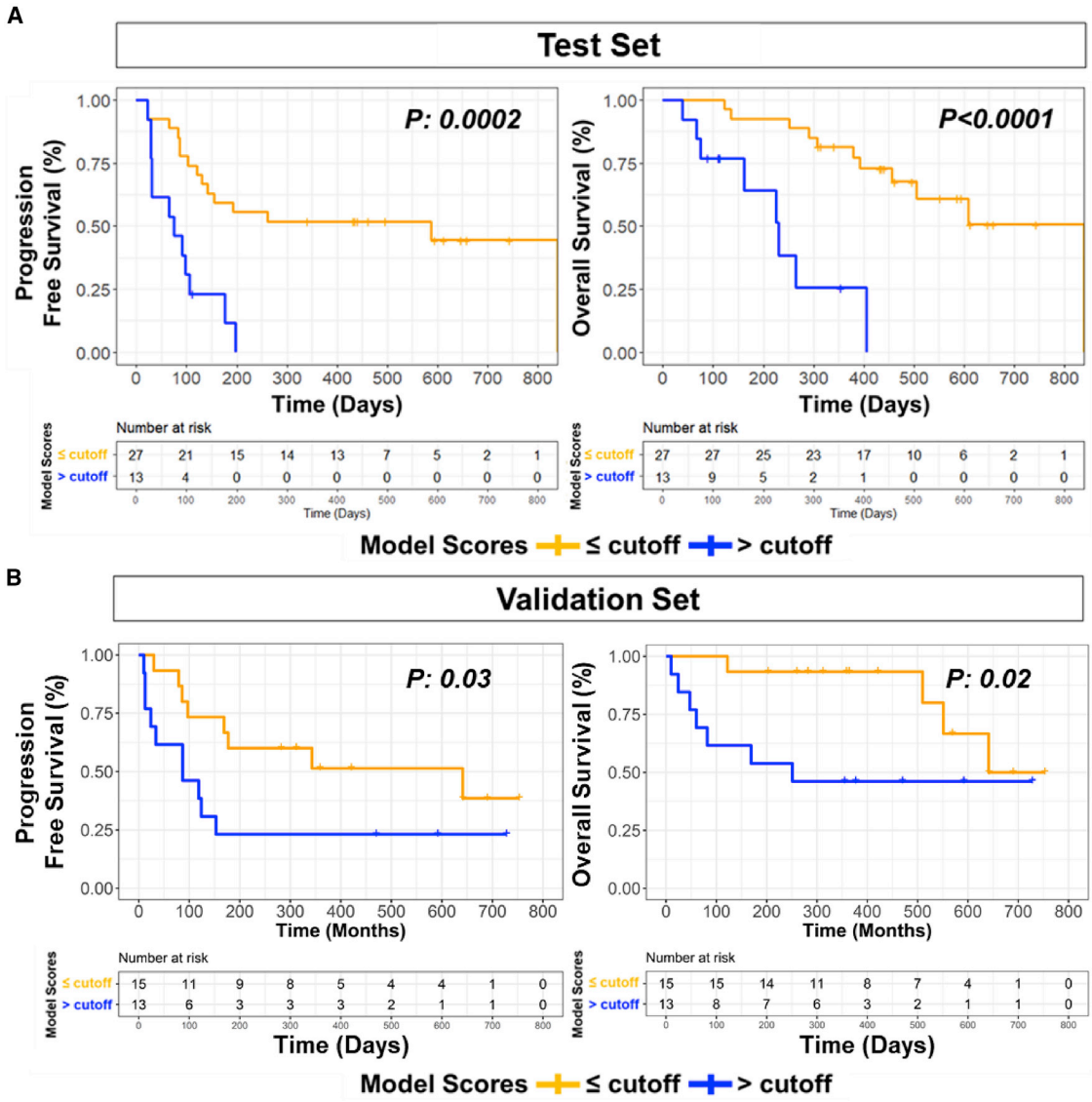

Figure 4. Association between 6MetP scores and PFS and OS in patients with B cell lymphoma treated with CAR-T

(A) Kaplan-Meier survival curves illustrate the association between the 6MetP > or ≤ an optimal cutoff value for prognosticating PFS and OS in the test set. The cutoff was established using log rank statistics[15] in the test set and represents the optimal cutoff value for prognosticating PFS. Mantel Cox log rank tests were used to compare differences in survival curves, and 2-sided p values are reported.

(B) Kaplan-Meier survival curves illustrate the association between the 6MetP > or ≤ an optimal cutoff value established in the test set for prognosticating PFS and OS in the validation set. Mantel Cox log rank tests were used to compare differences in survival curves, and 1-sided p values are reported.

SUPPLEMENTAL INFORMATION

Supplemental information can be found online at https://doi.org/10.1016/j.xcrm.2022.100720.

ACKNOWLEDGMENTS

This work was supported by the generous philanthropic contributions to the University of Texas MD Anderson Cancer Center Moon Shots Program and

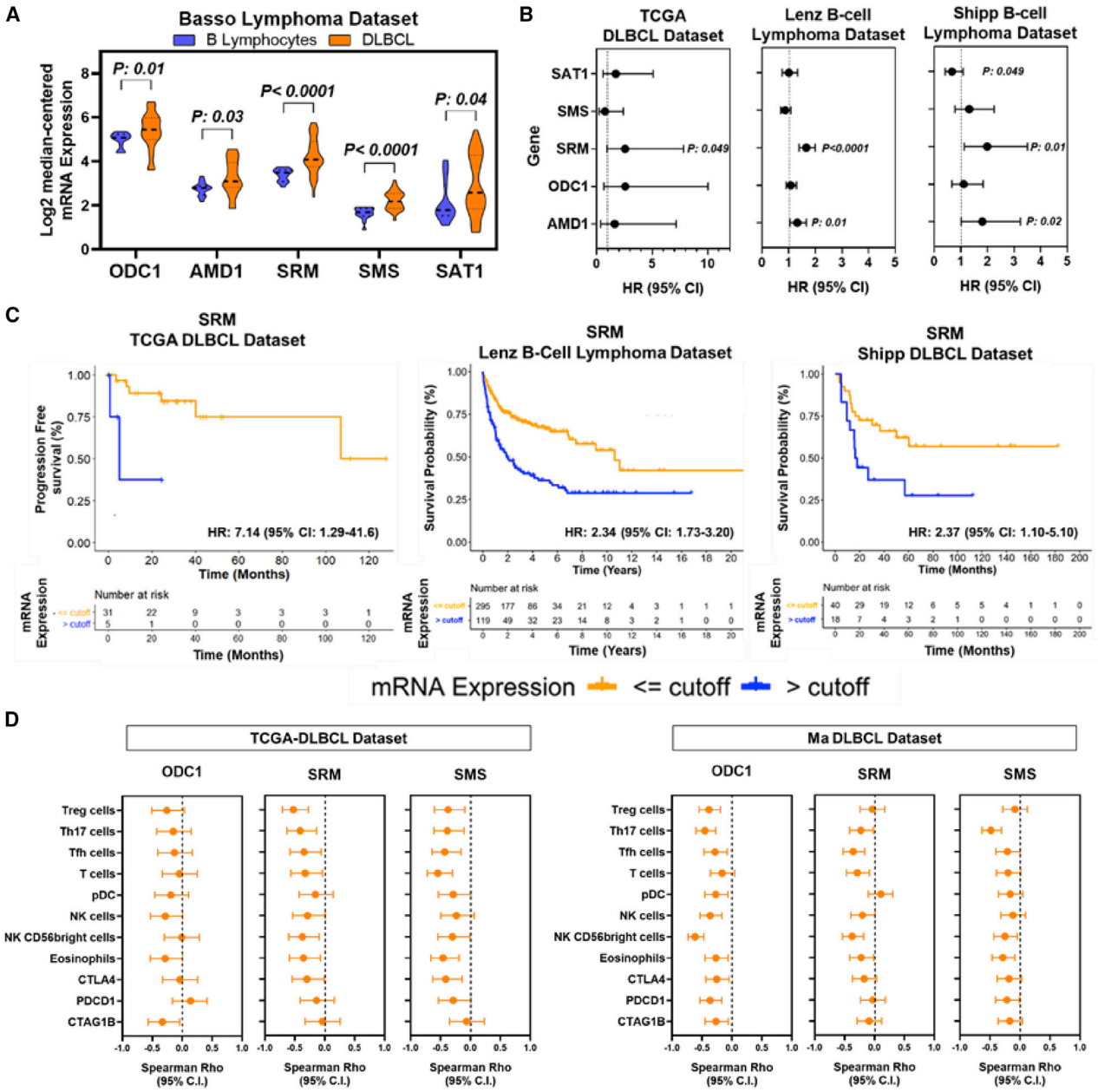

Figure 5. B cell lymphomas exhibit elevated mRNA expression of polyamine metabolizing enzymes and high spermidine synthase gene expression is prognostic for poor OS

(A) Violin plots illustrating mRNA expression of polyamine-metabolizing enzymes (PMEs) in diffuse large B cell lymphoma and normal B lymphocytes in the Basso lymphoma dataset.[16] Statistical significance was determined by 2-sided Wilcoxon rank sum test. ODC1, ornithine decarboxylase 1; AMD1, adenosylmethionine decarboxylase 1; SRM, spermidine synthase; SMS, spermine synthase; SAT1, spermidine/spermine N1-acetyltransferase 1.

(B) Dot plots illustrating HRs (95% CI) per unit increase in mRNA expression of PMEs, and PFS in The Cancer Genome Atlas (TCGA)-diffuse large B cell lymphoma (DLBCL) transcriptomic dataset and overall survival in the Lenz[17] and Shipp[18] B cell lymphoma transcriptomic datasets.

(C) Kaplan-Meier survival curves for association between mRNA expression of SRM > or $\leq$ an optimal change point value,[15] and PFS in the TCGA-DLBCL dataset and overall survival in the Lenz[17] and Shipp[18] B cell lymphoma datasets, respectively.

(D) Dot plots illustrate spearman ρ coefficients (95% CI) for association between mRNA expression of PMEs ODC1, SRM, and SMS with gene-based signatures of immune-cell infiltrates and immune-checkpoint-blockade-related genes in the TCGA-DLBCL and Ma DLBCL[19] transcriptomic datasets. Gene-based signatures were according to Bindea et al.[20] ODC1, ornithine decarboxylase 1; AMD1, adenosylmethionine decarboxylase 1; SRM, spermidine synthase; SMS, spermine synthase; SAT1, spermidine/spermine N1-acetyltransferase 1.

an NCI Cancer Center Support Grant to the University of Texas MD Anderson Cancer Center (P30 CA016672).

AUTHOR CONTRIBUTIONS

Conceptualization, J.F.F., N.Y.S., S.S.N., and S.H.; methodology, J.F.F., E.I., R.W., and J.B.D.; formal analysis, J.F.F. and E.I.; investigation, J.F.F. and N.Y.S.; resources: C.C.-C., P.S., R.N., L.E.F., S.A., H.J.L., S.I., R.S., L.N., P.J., M.W., M.G., J.W., V.B., M.D., R.C., E.J.S., P.K., C.R.F., M.J., R.J., C.K.S.-T., M.S., and S.S.N.; data curation, J.F.F., E.I., and R.W.; writing – original draft preparation, J.F.F. and N.Y.S.; writing – review & editing, C.C., E.I., P.S., R.N., L.E.F., S.A., H.J.L., S.I., R.S., J.V., R.W., J.B.D., L.N., P.J., M.W., M.G., J.W., V.B., M.D., R.C., E.J.S., P.K., C.R.F., M.J., R.J., C.K.S.-T., M.S., S.S.N., and S.H.; visualization: J.F.F. and E.I.; supervision: S.H.; project administration, S.S.N. and S.H.; funding acquisition: S.S.N.

DECLARATION OF INTERESTS

An Invention Disclosure Report related to findings reported herein has been submitted to the University of Texas. M.S. has received industry research support from Amgen, Gilead, Miltenyi Biotec, Morphosys, Roche, and Seattle Genetics and has served as a consultant/advisor to Amgen, BMS, Celgene, Gilead, Pfizer, Novartis, and Roche. She sits on the advisory boards of Amgen, Celgene, Gilead, Janssen, Novartis, Pfizer, and Seattle Genetics and serves on the speakers' bureau at Amgen, Celgene, Gilead, Janssen, and Pfizer. N.Y.S. has intellectual property rights in the field of cellular immunotherapy and microbiome. S.S.N. received personal fees from Kite, a Gilead Company, Merck, Bristol Myers Squibb, Novartis, Celgene, Pfizer, Allogene Therapeutics, Cell Medica/Kuur, Incyte, Precision Biosciences, Legend Biotech, Adicet Bio, Calibr, Bluebird Bio, and Unum Therapeutics; research support from Kite, a Gilead Company, Bristol Myers Squibb, Merck, Poseida, Cellectis, Celgene, Karus Therapeutics, Unum Therapeutics, Allogene Therapeutics, Precision Biosciences, and Acerta; royalties from Takeda Pharmaceuticals; and has intellectual property rights related to cell therapy. M.G. reports research funding from Sanofi, Kite/Gilead, Abbvie, and Allogene, honoraria from Tessa Therapeutics and Daiichi Sankyo, and stock ownership of KDAc Therapeutics. P.S. received research support from Astrazeneca-Acerta and from ALX Oncology and is a consultant for Roche-Genentech and Hutchinson MediPharma. S.S.N. has received personal fees from Kite, a Gilead Company, Merck, Bristol Myers Squibb, Novartis, Celgene, Pfizer, Allogene Therapeutics, Cell Medica/Kuur, Incyte, Precision Biosciences, Legend Biotech, Adicet Bio, Calibr, Unum Therapeutics, and Bluebird Bio; research support from Kite, a Gilead Company, Bristol Myers Squibb, Merck, Poseida, Cellectis, Celgene, Karus Therapeutics, Unum Therapeutics, Allogene Therapeutics, Precision Biosciences, and Acerta; and patents, royalties, or other intellectual property from Takeda Pharmaceuticals.

Received: November 23, 2021
Revised: June 6, 2022
Accepted: July 20, 2022
Published: August 16, 2022

REFERENCES

1. June, C.H., and Sadelain, M. (2018). Chimeric antigen receptor therapy. N. Engl. J. Med. *379*, 64–73. https://doi.org/10.1056/NEJMra1706169.
2. Neelapu, S.S., Locke, F.L., Bartlett, N.L., Lekakis, L.J., Miklos, D.B., Jacobson, C.A., Braunschweig, I., Oluwole, O.O., Siddiqi, T., Lin, Y., et al. (2017). Axicabtagene ciloleucel CAR T-cell therapy in refractory large B-cell lymphoma. N. Engl. J. Med. *377*, 2531–2544. https://doi.org/10.1056/NEJMoa1707447.
3. Schuster, S.J., Bishop, M.R., Tam, C.S., Waller, E.K., Borchmann, P., McGuirk, J.P., Jäger, U., Jaglowski, S., Andreadis, C., Westin, J.R., et al. (2019). Tisagenlecleucel in adult relapsed or refractory diffuse large B-cell lymphoma. N. Engl. J. Med. *380*, 45–56. https://doi.org/10.1056/NEJMoa1804980.
4. Abramson, J.S., Palomba, M.L., Gordon, L.I., Lunning, M.A., Wang, M., Arnason, J., Mehta, A., Purev, E., Maloney, D.G., Andreadis, C., et al. (2020). Lisocabtagene maraleucel for patients with relapsed or refractory large B-cell lymphomas (TRANSCEND NHL 001): a multicentre seamless design study. Lancet *396*, 839–852. https://doi.org/10.1016/S0140-6736(20)31366-0.
5. Vercellino, L., Di Blasi, R., Kanoun, S., Tessoulin, B., Rossi, C., D'Aveni-Piney, M., Obéric, L., Bodet-Milin, C., Bories, P., Olivier, P., et al. (2020). Predictive factors of early progression after CAR T-cell therapy in relapsed/refractory diffuse large B-cell lymphoma. Blood Adv. *4*, 5607–5615. https://doi.org/10.1182/bloodadvances.2020003001.
6. Jain, M.D., Zhao, H., Wang, X., Atkins, R., Menges, M., Reid, K., Spitler, K., Faramand, R., Bachmeier, C., Dean, E.A., et al. (2021). Tumor interferon signaling and suppressive myeloid cells are associated with CAR T-cell failure in large B-cell lymphoma. Blood *137*, 2621–2633. https://doi.org/10.1182/blood.2020007445.
7. Ott, G., Rosenwald, A., and Campo, E. (2013). Understanding MYC-driven aggressive B-cell lymphomas: pathogenesis and classification. Blood *122*, 3884–3891. https://doi.org/10.1182/blood-2013-05-498329.
8. Ziepert, M., Lazzi, S., Santi, R., Vergoni, F., Granai, M., Mancini, V., Staiger, A., Horn, H., Löffler, M., Pöschel, V., et al. (2020). A 70% cut-off for MYC protein expression in diffuse large B cell lymphoma identifies a high-risk group of patients. Haematologica *105*, 2667–2670. https://doi.org/10.3324/haematol.2019.235556.
9. Jaeger, U., Bishop, M.R., Salles, G., Schuster, S.J., Maziarz, R.T., Han, X., Savchenko, A., Roscoe, N., Orlando, E., Knoblock, D., et al. (2020). Myc expression and tumor-infiltrating T cells are associated with response in patients (Pts) with relapsed/refractory diffuse large B-cell lymphoma (r/r DLBCL) treated with tisagenlecleucel in the juliet trial. Blood *136*, 48–49. https://doi.org/10.1182/blood-2020-137045.
10. Fahrmann, J.F., Bantis, L.E., Capello, M., Scelo, G., Dennison, J.B., Patel, N., Murage, E., Vykoukal, J., Kundnani, D.L., Foretova, L., et al. (2019). A plasma-derived protein-metabolite multiplexed panel for early-stage pancreatic cancer. J. Natl. Cancer Inst. *111*, 372–379. https://doi.org/10.1093/jnci/djy126.
11. Fahrmann, J.F., Vykoukal, J., Fleury, A., Tripathi, S., Dennison, J.B., Murage, E., Wang, P., Yu, C.Y., Capello, M., Creighton, C.J., et al. (2020). Association between plasma diacetylspermine and tumor spermine synthase with outcome in triple-negative breast cancer. J. Natl. Cancer Inst. *112*, 607–616. https://doi.org/10.1093/jnci/djz182.
12. Fahrmann, J.F., Irajizad, E., Kobayashi, M., Vykoukal, J., Dennison, J.B., Murage, E., Wu, R., Long, J.P., Do, K.A., Celestino, J., et al. (2021). A MYC-driven plasma polyamine signature for early detection of ovarian cancer. Cancers (Basel) *13*, 913. https://doi.org/10.3390/cancers13040913.
13. Kühn, T., Floegel, A., Sookthai, D., Johnson, T., Rolle-Kampczyk, U., Otto, W., von Bergen, M., Boeing, H., and Kaaks, R. (2016). Higher plasma levels of lysophosphatidylcholine 18:0 are related to a lower risk of common cancers in a prospective metabolomics study. BMC Med *14*, 13. https://doi.org/10.1186/s12916-016-0552-3.
14. Zhao, Z., Xiao, Y., Elson, P., Tan, H., Plummer, S.J., Berk, M., Aung, P.P., Lavery, I.C., Achkar, J.P., Li, L., et al. (2007). Plasma lysophosphatidylcholine levels: potential biomarkers for colorectal cancer. J. Clin. Oncol. *25*, 2696–2701. https://doi.org/10.1200/jco.2006.08.5571.
15. Contal, C., and O'Quigley, J. (1999). An application of changepoint methods in studying the effect of age on survival in breast cancer. Comput. Stat. Data Anal. *30*, 253–270.
16. Basso, K., Margolin, A.A., Stolovitzky, G., Klein, U., Dalla-Favera, R., and Califano, A. (2005). Reverse engineering of regulatory networks in human B cells. Nat. Genet. *37*, 382–390. https://doi.org/10.1038/ng1532.
17. Lenz, G., Wright, G., Dave, S.S., Xiao, W., Powell, J., Zhao, H., Xu, W., Tan, B., Goldschmidt, N., Iqbal, J., et al. (2008). Stromal gene signatures in large-B-cell lymphomas. N. Engl. J. Med. *359*, 2313–2323. https://doi.org/10.1056/NEJMoa0802885.

18. Shipp, M.A., Ross, K.N., Tamayo, P., Weng, A.P., Kutok, J.L., Aguiar, R.C.T., Gaasenbeek, M., Angelo, M., Reich, M., Pinkus, G.S., et al. (2002). Diffuse large B-cell lymphoma outcome prediction by gene-expression profiling and supervised machine learning. Nat. Med. *8*, 68–74. https://doi.org/10.1038/nm0102-68.

19. Ma, M.C.J., Tadros, S., Bouska, A., Heavican, T.B., Yang, H., Deng, Q., Moore, D., Akhter, A., Hartert, K., Jain, N., et al. (2019). Pathognomonic and epistatic genetic alterations in B-cell non-Hodgkin lymphoma. Preprint at bioRxiv, 674259. https://doi.org/10.1101/674259.

20. Bindea, G., Mlecnik, B., Tosolini, M., Kirilovsky, A., Waldner, M., Obenauf, A.C., Angell, H., Fredriksen, T., Lafontaine, L., Berger, A., et al. (2013). Spatiotemporal dynamics of intratumoral immune cells reveal the immune landscape in human cancer. Immunity *39*, 782–795. https://doi.org/10.1016/j.immuni.2013.10.003.

21. Shah, N.N., and Fry, T.J. (2019). Mechanisms of resistance to CAR T cell therapy. Nat. Rev. Clin. Oncol. *16*, 372–385. https://doi.org/10.1038/s41571-019-0184-6.

22. Nastoupil, L.J., Jain, M.D., Feng, L., Spiegel, J.Y., Ghobadi, A., Lin, Y., Dahiya, S., Lunning, M., Lekakis, L., Reagan, P., et al. (2020). Standard-of-Care axicabtagene ciloleucel for relapsed or refractory large B-cell lymphoma: results from the US lymphoma CAR T consortium. J. Clin. Oncol. *38*, 3119–3128. https://doi.org/10.1200/jco.19.02104.

23. Thyss, A., Milano, G., Caldani, C., Lesbats, G., Schneider, M., and Lalanne, C.M. (1982). Polyamines as biological markers in malignant lymphomas. Eur. J. Cancer Clin. Oncol. *18*, 611–616. https://doi.org/10.1016/0277-5379(82)90205-x.

24. Flynn, A.T., and Hogarty, M.D. (2018). Myc, oncogenic protein translation, and the role of polyamines. Med Sci (Basel) *6*. https://doi.org/10.3390/medsci6020041.

25. Coleman, C.S., Stanley, B.A., Jones, A.D., and Pegg, A.E. (2004). Spermidine/spermine-N1-acetyltransferase-2 (SSAT2) acetylates thialysine and is not involved in polyamine metabolism. Biochem J *384*, 139–148. https://doi.org/10.1042/bj20040790.

26. Bonaventura, P., Shekarian, T., Alcazer, V., Valladeau-Guilemond, J., Valsesia-Wittmann, S., Amigorena, S., Caux, C., and Depil, S. (2019). Cold tumors: a therapeutic challenge for immunotherapy. Front. Immunol. *10*, 168. https://doi.org/10.3389/fimmu.2019.00168.

27. Majzner, R.G., and Mackall, C.L. (2018). Tumor antigen escape from CAR T-cell therapy. Cancer Discov. *8*, 1219–1226. https://doi.org/10.1158/2159-8290.Cd-18-0442.

28. Alexander, E.T., Mariner, K., Donnelly, J., Phanstiel, O., 4th, and Gilmour, S.K. (2020). Polyamine blocking therapy decreases survival of tumor-infiltrating immunosuppressive myeloid cells and enhances the antitumor efficacy of PD-1 blockade. Mol. Cancer Therapeut. *19*, 2012–2022. https://doi.org/10.1158/1535-7163.Mct-19-1116.

29. Alexander, E.T., Minton, A., Peters, M.C., Phanstiel, O.t., and Gilmour, S.K. (2017). A novel polyamine blockade therapy activates an anti-tumor immune response. Oncotarget *8*, 84140–84152. https://doi.org/10.18632/oncotarget.20493.

30. Hayes, C.S., Shicora, A.C., Keough, M.P., Snook, A.E., Burns, M.R., and Gilmour, S.K. (2014). Polyamine-blocking therapy reverses immunosuppression in the tumor microenvironment. Cancer Immunol. Res. *2*, 274–285. https://doi.org/10.1158/2326-6066.Cir-13-0120-t.

31. Miska, J., Rashidi, A., Lee-Chang, C., Gao, P., Lopez-Rosas, A., Zhang, P., Burga, R., Castro, B., Xiao, T., Han, Y., et al. (2021). Polyamines drive myeloid cell survival by buffering intracellular pH to promote immunosuppression in glioblastoma. Sci. Adv. *7*, eabc8929. https://doi.org/10.1126/sciadv.abc8929.

32. Edwards-Hicks, J., Mitterer, M., Pearce, E.L., and Buescher, J.M. (2021). Metabolic dynamics of *in vitro* CD8+ T cell activation. Metabolites *11*, 12.

33. O'Brien, K.L., Assmann, N., O'Connor, E., Keane, C., Walls, J., Choi, C., Oefner, P.J., Gardiner, C.M., Dettmer, K., and Finlay, D.K. (2021). De novo polyamine synthesis supports metabolic and functional responses in activated murine NK cells. European Journal of Immunology *51*, 91–102.

34. Puleston, D.J., Baixauli, F., Sanin, D.E., Villa, M., Kabat, A., Kamiński, M.M., Weiss, H., Grzes, K., Flachsmann, L., and Field, C.S. (2020). Polyamine metabolism regulates the T cell epigenome through hypusination. Preprint at bioRxiv.

35. Sholler, G.L.S., Ferguson, W., Bergendahl, G., Bond, J.P., Neville, K., Eslin, D., Brown, V., Roberts, W., Wada, R.K., Oesterheld, J., et al. (2018). Maintenance DFMO increases survival in high risk neuroblastoma. Sci. Rep. *8*, 14445. https://doi.org/10.1038/s41598-018-32659-w.

36. Samal, K., Zhao, P., Kendzicky, A., Yco, L.P., McClung, H., Gerner, E., Burns, M., Bachmann, A.S., and Sholler, G. (2013). AMXT-1501, a novel polyamine transport inhibitor, synergizes with DFMO in inhibiting neuroblastoma cell proliferation by targeting both ornithine decarboxylase and polyamine transport. Int. J. Cancer *133*, 1323–1333. https://doi.org/10.1002/ijc.28139.

37. Kamphorst, J.J., Cross, J.R., Fan, J., de Stanchina, E., Mathew, R., White, E.P., Thompson, C.B., and Rabinowitz, J.D. (2013). Hypoxic and Ras-transformed cells support growth by scavenging unsaturated fatty acids from lysophospholipids. Proc. Natl. Acad. Sci. USA. *110*, 8882–8887. https://doi.org/10.1073/pnas.1307237110.

38. Raynor, A., Jantscheff, P., Ross, T., Schlesinger, M., Wilde, M., Haasis, S., Dreckmann, T., Bendas, G., and Massing, U. (2015). Saturated and mono-unsaturated lysophosphatidylcholine metabolism in tumour cells: a potential therapeutic target for preventing metastases. Lipids Health Dis. *14*, 69. https://doi.org/10.1186/s12944-015-0070-x.

39. Piccirillo, A.R., Hyzny, E.J., Beppu, L.Y., Menk, A.V., Wallace, C.T., Hawse, W.F., Buechel, H.M., Wong, B.H., Foo, J.C., Cazenave-Gassiot, A., et al. (2019). The lysophosphatidylcholine transporter MFSD2A is essential for CD8(+) memory T cell maintenance and secondary response to infection. J. Immunol. *203*, 117–126. https://doi.org/10.4049/jimmunol.1801585.

40. Asaoka, Y., Oka, M., Yoshida, K., Sasaki, Y., and Nishizuka, Y. (1992). Role of lysophosphatidylcholine in T-lymphocyte activation: involvement of phospholipase A2 in signal transduction through protein kinase C. Proc. Natl. Acad. Sci. USA. *89*, 6447–6451. https://doi.org/10.1073/pnas.89.14.6447.

41. Mollinedo, F., de la Iglesia-Vicente, J., Gajate, C., Estella-Hermoso de Mendoza, A., Villa-Pulgarin, J.A., de Frias, M., Roué, G., Gil, J., Colomer, D., Campanero, M.A., and Blanco-Prieto, M.J. (2010). *In vitro* and *in vivo* selective antitumor activity of Edelfosine against mantle cell lymphoma and chronic lymphocytic leukemia involving lipid rafts. Clin. Cancer Res. *16*, 2046–2054. https://doi.org/10.1158/1078-0432.Ccr-09-2456.

42. Estella-Hermoso de Mendoza, A., Campanero, M.A., de la Iglesia-Vicente, J., Gajate, C., Mollinedo, F., and Blanco-Prieto, M.J. (2009). Antitumor alkyl ether lipid edelfosine: tissue distribution and pharmacokinetic behavior in healthy and tumor-bearing immunosuppressed mice. Clin. Cancer Res. *15*, 858–864. https://doi.org/10.1158/1078-0432.Ccr-08-1654.

43. Gajate, C., and Mollinedo, F. (2007). Edelfosine and perifosine induce selective apoptosis in multiple myeloma by recruitment of death receptors and downstream signaling molecules into lipid rafts. Blood *109*, 711–719. https://doi.org/10.1182/blood-2006-04-016824.

44. Cheson, B.D., Fisher, R.I., Barrington, S.F., Cavalli, F., Schwartz, L.H., Zucca, E., and Lister, T.A.Alliance, Australasian Leukaemia and Lymphoma Group; Eastern Cooperative Oncology Group; European Mantle Cell Lymphoma Consortium (2014). Recommendations for initial evaluation, staging, and response assessment of Hodgkin and non-Hodgkin lymphoma: the Lugano classification. J. Clin. Oncol. *32*, 3059–3068. https://doi.org/10.1200/jco.2013.54.8800.

45. Neelapu, S.S., Tummala, S., Kebriaei, P., Wierda, W., Gutierrez, C., Locke, F.L., Komanduri, K.V., Lin, Y., Jain, N., Daver, N., et al. (2018). Chimeric antigen receptor T-cell therapy - assessment and management of toxicities.

Nat. Rev. Clin. Oncol. *15*, 47–62. https://doi.org/10.1038/nrclinonc.2017.148.

46. Vykoukal, J., Fahrmann, J.F., Gregg, J.R., Tang, Z., Basourakos, S., Irajizad, E., Park, S., Yang, G., Creighton, C.J., Fleury, A., et al. (2020). Caveolin-1-mediated sphingolipid oncometabolism underlies a metabolic vulnerability of prostate cancer. Nat. Commun. *11*, 4279. https://doi.org/10.1038/s41467-020-17645-z.

47. Gao, J., Aksoy, B.A., Dogrusoz, U., Dresdner, G., Gross, B., Sumer, S.O., Sun, Y., Jacobsen, A., Sinha, R., Larsson, E., et al. (2013). Integrative analysis of complex cancer genomics and clinical profiles using the cBioPortal. Sci. Signal. *6*, pl1. https://doi.org/10.1126/scisignal.2004088.

48. Rhodes, D.R., Yu, J., Shanker, K., Deshpande, N., Varambally, R., Ghosh, D., Barrette, T., Pandey, A., and Chinnaiyan, A.M. (2004). ONCOMINE: a cancer microarray database and integrated data-mining platform. Neoplasia *6*, 1–6. https://doi.org/10.1016/s1476-5586(04)80047-2.

49. Friedman, J., Hastie, T., and Tibshirani, R. (2010). Regularization paths for generalized linear models via coordinate descent. J. Stat. Softw. *33*, 1–22.

50. Grambsch, P.M., and Therneau, T.M. (1994). Proportional hazards tests and diagnostics based on weighted residuals. Biometrika *81*, 515–526. https://doi.org/10.1093/biomet/81.3.515.

STAR★METHODS

KEY RESOURCES TABLE

REAGENT or RESOURCE	SOURCE	IDENTIFIER
Biological samples		
Plasmas from individuals with r/r LBCL that subsequently received anti-CD19 CAR-T treatment	University of Texas MD Anderson Cancer Center, Texas, USA	IRB Protocol: LAB04-0717
Serum samples from individuals with r/r LBCL that subsequently received anti-CD19 CAR-T treatment	German Cancer Research Institute, Heidelberg, Germany	
Deposited data		
MetaboLights	This paper	https://www.ebi.ac.uk/metabolights/MTBLS5381/
Other		
Acquity™ UPLC BEH amide, 100 Å, 1.7 μm 2.1 × 100 mm column	Waters Corporation, Milford, USA	catalog number: 176,001,908
Acquity™ UPLC HSS T3, 100 Å, 1.8 μm, 2.1 × 100 mm column	Waters Corporation, Milford, USA	catalog number: 176001132
Ammonium formate (optima LCMS)	ThermoFisher, Waltham, MA, USA	catalog number: A11550
Formic Acid	Honeywell Fluka, Charlotte, NC, USA	catalog number: 60-006-17
LCMS Grade Acetonitrile	ThermoFisher, Waltham, MA, USA	catalog number: A955-4
LCMS Grade Methanol	ThermoFisher, Waltham, MA, USA	catalog number: A456-4
LCMS Grade Isopropanol	ThermoFisher, Waltham, MA, USA	catalog number: A461-4
The Cancer Genome Atlas DLBCL Transcriptomic Dataset	http://www.cbioportal.org/	TCGA, PanCancer Atlas
Ma B-Cell Malignancies Transcriptomic Dataset	http://www.cbioportal.org/	Ma et al., 2019
Basso Lymphoma Transcriptomic Dataset	https://www.oncomine.org/resource/login.html	Basso et al., 2005
Lenz B-cell Lymphoma Transcriptomic Dataset	https://www.oncomine.org/resource/login.html	Lenz et al., 2008
Shipp B-cell Lymphoma Transcriptomic Dataset	https://www.oncomine.org/resource/login.html	Shipp et al., 2002

RESOURCE AVAILABILITY

Lead contact

Further information and requests for resources and reagents should be direct to and will be fulfilled by the lead contact, Samir Hanash, M.D., Ph.D. (shanash@mdanderson.org).

Materials availability

This study did not generate new reagents. There are restrictions to the availability of human biospecimens due to existing MTA.

Data and code availability

- Relevant data supporting the findings of this study are available within the Article and Supplemental Materials.
- No new code was generated for this study.
- Any additional information required to reanalyze the data reported in this paper is available from the lead contact upon request.

EXPERIMENTAL MODEL AND SUBJECT DETAILS

Human subjects

The human plasma and serum samples were collected through an international collaboration between MD Anderson Cancer Center (MDACC), Houston, USA, and German Cancer Research Center (DKFZ), Heidelberg, Germany. The clinical data and patient's serum samples were collected under existing Institutional Research Board (IRB) approved protocols at each center and conducted in accordance with institutional guidelines and the principles of the Declaration of Helsinki. All participants had consent for the use of samples in ethically approved studies. Response status was determined by Lugano 2014 classification.[44] Cytokine release syndrome (CRS)

and immune effector cell-associated neurotoxicity syndrome (ICANS) were prospectively graded and managed according to the CAR T-cell therapy associated toxicity guidelines.[45] For MDACC cohort analysis, plasma samples were obtained from 43 sequential r/r LBCL patients before they received CAR T-cell infusion as a standard of care product. Of the 43 samples, 39 were collected on the day of treatment (day 0) and the remaining 4 were collected within 4 days prior to CAR T-cell therapy. Patients who were enrolled in CAR T-cell clinical trials were excluded from the study. For validation purpose, serum samples obtained on day of treatment prior to CAR T-cell infusion from another 28 patients from German (DKFZ) r/r LBCL cohort were analyzed.

METHOD DETAILS

Assessment of MYC rearrangement and protein expression

Information regarding MYC rearrangement and protein expression was obtained from the pathology report documented in the electronic medical record. Fluorescence *in situ* hybridization (FISH) analysis was used to determine *MYC*, *BCL2*, and *BCL6* gene rearrangements. For *MYC* rearrangement detection, a MYC dual color break apart rearrangement probe located at 8q24.2 (Abbott Molecular) was used – 5'MYC – centromeric (spectrum orange)/3'MYC- telomeric (spectrum green). The cutoff for positivity of MYC rearrangement at MDACC pathology lab is 8.1%. For MYC protein expression, lymphoma tissue was stained with anti-c-MYC (Ventana, Cat # 790-4628) and results documented as percentage of cells positive for c-MYC expression.

Metabolomic analysis

Sample extraction

Primary metabolites and biogenic amines. Plasma and serum metabolites were extracted from pre-aliquoted biospecimens (15μL) with 45μL of LCMS grade methanol (ThermoFisher) in a 96-well microplate (Eppendorf). Plates were heat sealed, vortexed for 5 min at 750 rpm, and centrifuged at 2000 × g for 10 min at room temperature. The supernatant (30μL) was carefully transferred to a 96-well plate, leaving behind the precipitated protein. The supernatant was further diluted with 60μL of 100 mM ammonium formate, pH3 (Fisher Scientific). For Hydrophilic Interaction Liquid Chromatography (HILIC) positive ion analysis, 15μL of the supernatant and ammonium formate mix were diluted with 195μL of 1:3:8:144 water (GenPure ultrapure water system, Thermofisher): LCMS grade methanol (ThermoFisher): 100 mM ammonium formate, pH3 (Fisher Scientific): LCMS grade acetonitrile (ThermoFisher). For the HILIC negative ion analysis, 15μL of the supernatant and ammonium formate mix were diluted with 90μL of LCMS grade acetonitrile (ThermoFisher). For C18 analysis, 15μL of the supernatant and ammonium formate mix were diluted with 90μL water (GenPure ultrapure water system, ThermoFisher) for positive and negative ion modes, respectively. Each sample solution was transferred to 384-well microplate (Eppendorf) for LCMS analysis.

Complex lipids. Pre-aliquoted serum or plasma samples (10μL) were extracted with 30μL of LCMS grade 2-propanol (ThermoFisher) in a 96-well microplate (Eppendorf). Plates were heat sealed, vortexed for 5 min at 750 rpm, and centrifuged at 2000 x g for 10 min at room temperature. The supernatant (10μL) was carefully transferred to a 96-well plate, leaving behind the precipitated protein. The supernatant was further diluted with 90μL of 1:3:2 100 mM ammonium formate, pH3 (Fischer Scientific): LCMS grade acetonitrile (ThermoFisher): LCMS grade 2-propanol (ThermoFisher) and transferred to a 384-well microplate (Eppendorf) for lipids analysis using LCMS.

Untargeted analysis of primary metabolites and biogenic amines. Untargeted metabolomics analysis was conducted on Waters Acquity™ UPLC system with 2D column regeneration configuration (I-class and H-class) coupled to a Xevo G2-XS quadrupole time-of-flight (qTOF) mass spectrometer. Chromatographic separation was performed using HILIC (Acquity™ UPLC BEH amide, 100 Å, 1.7 μm 2.1 × 100 mm, Waters Corporation, Milford, U.S.A) and C18 (Acquity™ UPLC HSS T3, 100 Å, 1.8 μm, 2.1 × 100 mm, Water Corporation, Milford, U.S.A) columns at 45°C.

Quaternary solvent system mobile phases were (A) 0.1% formic acid in water, (B) 0.1% formic acid in acetonitrile and (D) 100 mM ammonium formate, pH 3. Samples were separated using the following gradient profile: for the HILIC separation a starting gradient of 95% B and 5% D was linearly changed to 70% A, 25% B and 5% D over a 5 min period at 0.4 mL/min flow rate, and to 100% A over 1 min, followed by another 1 min isocratic gradient at 100 % A at 0.4 mL/min flow rate to initiate the starting gradient for the next C18 run. For C18 separation, the chromatography gradient was as follows: starting conditions, 100% A, with a linear change to 5% A, 95% B over a 5 min period at 0.4 mL/min flow rate, reverted back to 95% B, 5% D over 1 min, and then followed by 1 min isocratic gradient at 95% B, 5% D at 0.4 mL/min for the next HILIC run.

A binary pump was used for column regeneration and equilibration. The solvent system mobile phases were (A1) 100 mM ammonium formate, pH 3, (A2) 0.1% formic in 2-propanol and (B1) 0.1% formic acid in acetonitrile. The HILIC column was stripped using 90% A2 for 5 min at 0.25 mL/min flow rate, followed by a 2 min equilibration using 100% B1 at 0.3 mL/min flow rate. Reverse phase C18 column regeneration was performed using 95% A1, 5% B1 for 2 min followed by column equilibration using 5% A1, 95% B1 for 5 min at 0.4 mL/min flow rate.

Untargeted analysis of complex lipids. For the lipidomic assay, untargeted metabolomics analysis was conducted on a Waters Acquity UPLC system coupled to a Xevo G2-XS quadrupole time-of-flight (qTOF) mass spectrometer. Chromatographic separation was performed using a C18 (Acquity™ UPLC HSS T3, 100 Å, 1.8 μm, 2.1 × 100 mm, Water Corporation, Milford, U.S.A) column at 55°C. The mobile phases were (A) water, (B) acetonitrile, (C) 2-propanol and (D) 500 mM ammonium formate, pH 3. A starting elution gradient of 20% A, 30% B, 49% C and 1% D was linearly changed to 4% A, 14% B, 81% C and 1% D for4.5 min, followed by isocratic elution at 4% A,14% B, 81% C and 1%D for 2.1 min and column equilibration with initial conditions for 1.4 min.

Mass spectrometry data acquisition. Mass spectrometry data was acquired using 'sensitivity' mode in positive and negative electrospray ionization mode within 50–800 Da range for primary metabolites and 100–2000 Da for complex lipids. For the electrospray acquisition, the capillary voltage was set at 1.5 kV (positive), 3.0 kV (negative), sample cone voltage 30 V, source temperature at 120°C, cone gas flow 50 L/h and desolvation gas flow rate of 800 L/h with scan time of 0.5 sec in continuum mode. Leucine Enkephalin; 556.2771 Da (positive) and 554.2615 Da (negative) was used for lockspray correction and scans were performed at 0.5sec. The injection volume for each sample was 3μL for complex lipids, and 6μL for primary metabolites. The acquisition was carried out with instrument auto gain control to optimize instrument sensitivity over the samples acquisition time.

Data were processed using Progenesis QI (Nonlinear, Waters). Peak picking and retention time alignment of LC-MS and MSe data were performed using Progenesis QI software (Nonlinear, Waters). Data processing and peak annotations were performed using an in-house automated pipeline as previously described.[10–12,46] Annotations were determined by matching accurate mass and retention times using customized libraries created from authentic standards and by matching experimental tandem mass spectrometry data against the NIST MSMS, LipidBlast or HMDB v3 theoretical fragmentations; for complex lipids retention time patterns characteristic of lipid subclasses was also considered. To correct for injection order drift, each feature was normalized using data from repeat injections of quality control samples collected every 10 injections throughout the run sequence. Measurement data were smoothed by Locally Weighted Scatterplot Smoothing (LOESS) signal correction (QC-RLSC) as previously described. Values are reported as ratios relative to the median of historical quality control reference samples run with every analytical batch for the given analyte.[10–12,46]

Gene expression datasets

Gene expression data for primary treatment-naïve LBCLs and associated clinical information from The Cancer Genome Atlas (TCGA)-DLBCL and the Ma B-Cell malignancies[19] datasets were downloaded from cbioportal.[47] Gene expression data and associated clinical information for the Basso Lymphoma,[16] Lenz B-cell lymphoma,[17] and Shipp B-Cell lymphoma[18] datasets were downloaded from Oncomine database.[48] The identifies of specific immune cell infiltrations were computationally inferred using RNA-seq data based on gene sets overexpressed in one of 24 immune cell types, according to Bindea et al.[20]

Statistical analysis

For data analysis, we use PFS as our primary outcome of interest. Cox proportional hazard models with Least Absolute Shrinkage and Selection Operator (LASSO) regularization using glmnet package in R statistical software[49] were used to select metabolite features and develop a biomarker panel for predicting PFS. LASSO in the cox regression adds a constraint to the optimization function. Here, the Cox model assumes a semi-parametric form for the assumes a semi-parametric form for the hazard:

$$h_i(t) = h_0(t)e^{x_i^t\beta}$$

where $h_i(t)$is the hazard for patient i at time t, $h_0(t)$is a shared baseline hazard, and β is a vector of size p (p = number of features in our samples).

The corresponding partial likelihood to maximize for the cox equation is:

$$L(\beta) = \prod_{i=1}^{m} \frac{e^{x_{j(i)}^t\beta}}{\sum_{j\in R_i} e^{x_j^t\beta}}$$

R_i is the set of indices, j, with $y_j \geq t_i$ (those at risk at time t_i). This equation subjects to the following constrain:

$$\alpha\sum|\beta_j| + (1-\alpha)\sum\beta_j^2 \leq c$$

$\alpha = 1$ gives the lasso penalty in these equations.

βs that are deemed not important in the likelihood function are shrunk to be zero, resulting in a simplified regression model.

Coefficients of the selected features were derived in the Test Set and applied to the Validation Set. To test for the proportionality of Hazard assumption of a Cox regression, we utilized the method of Patricia et al.[50]

Log rank statistic based methods as described by Contal and O'Quigley[15] were used to determine optimal cutoff value for the model to distinguish patients that had progressive disease from those that had a complete response following CAR-T treatment. Kaplan-Meier survival analyses were performed using R Version 1.1.442. Log-rank (Mantel-Cox) tests were used to assess for statistical differences between survival curves.

Linear mixed models with random intercept and slope were incorporated to calculate the association between polyamine levels following CAR-T infusion. Reported values (slope and intercepts) are the average representation of all calculated coefficients for each patient. P-values were calculated from 10,000 bootstraps of the delta value between responders and non-responders.

Area under the Receiver Operating Characteristic curves (AUC) were generated using R (R version 3.6.0). The 95% confidence intervals presented for individual performance of each biomarker were based on the bootstrap procedure in which we re-sampled with replacement 1000 times. For two-class comparisons, statistical significance was determined using Wilcoxon rank sum test. Statistical significance was determined at p-values <0.05 for all analyses unless otherwise stated. Figures were generated in Graph Pad Prism Version 8.0 (GraphPad Software, Inc. San Diego, CA, USA).